



A CpG Methylation Signature as a Potential Marker for Early Diagnosis of Hepatocellular Carcinoma From HBV-Related Liver Disease Using Multiplex Bisulfite Sequencing

OPEN ACCESS

Kang Li^{1†}, Yi Song^{2†}, Ling Qin¹, Ang Li¹, Sanjie Jiang³, Lei Ren⁴, Chaoran Zang¹, Jianping Sun¹, Yan Zhao⁵ and Yonghong Zhang^{1*}

Edited by:

Yuming Jiang,
Stanford University, United States

Reviewed by:

Ao Ren,
First Affiliated Hospital of Chongqing
Medical University, China
Nghiem Xuan Hoan,
108 Hospital, Vietnam

*Correspondence:

Yonghong Zhang
zhangyh@ccmu.edu.cn

[†]These authors have contributed
equally to this work

Specialty section:

This article was submitted to
Gastrointestinal Cancers: Hepato
Pancreatic Biliary Cancers,
a section of the journal
Frontiers in Oncology

Received: 11 August 2021

Accepted: 27 September 2021

Published: 20 October 2021

Citation:

Li K, Song Y, Qin L, Li A, Jiang S,
Ren L, Zang C, Sun J, Zhao Y and
Zhang Y (2021) A CpG Methylation
Signature as a Potential Marker for
Early Diagnosis of Hepatocellular
Carcinoma From HBV-Related
Liver Disease Using Multiplex
Bisulfite Sequencing.
Front. Oncol. 11:756326.
doi: 10.3389/fonc.2021.756326

¹ Biomedical Information Center, Beijing You'An Hospital, Capital Medical University, Beijing, China, ² Experimental Center, Beijing Friendship Hospital, Capital Medical University, Beijing, China, ³ St. Edmunds College, Cambridge, United Kingdom, ⁴ Pharmacology Department, Air Force Medical Center, People's Liberation Army of China (PLA), Beijing, China, ⁵ Clinical Laboratory Center, Beijing You'An Hospital, Capital Medical University, Beijing, China

Background: Aberrant methylation of CpG sites served as an epigenetic marker for building diagnostic, prognostic, and recurrence models for hepatocellular carcinoma (HCC).

Methods: Using Illumina 450K and EPIC Beadchip, we identified 34 CpG sites in peripheral blood mononuclear cell (PBMC) DNA that were differentially methylated in early HCC versus HBV-related liver diseases (HBVLD). We employed multiplex bisulfite sequencing (MBS) based on next-generation sequencing (NGS) to measure methylation of 34 CpG sites in PBMC DNA from 654 patients that were divided into a training set ($n = 442$) and a test set ($n = 212$). Using the training set, we selected and built a six-CpG-scorer (namely, cg14171514, cg07721852, cg05166871, cg18087306, cg05213896, and cg18772205), applying least absolute shrinkage and selection operator (LASSO) regression. We performed multivariable analyses of four candidate risk predictors (namely, six-CpG-scorer, age, sex, and AFP level), using 20 times imputation of missing data, non-linearly transformed, and backwards feature selection with logistic regression. The final model's regression coefficients were calculated according to "Rubin's Rules". The diagnostic accuracy of the model was internally validated with a 10,000 bootstrap validation dataset and then applied to the test set for validation.

Results: The area under the receiver operating characteristic curve (AUROC) of the model was 0.81 (95% CI, 0.77–0.85) and it showed good calibration and decision curve analysis. Using enhanced bootstrap validation, adjusted C-statistics and adjusted Brier score were 0.809 and 0.199, respectively. The model also showed an AUROC value of 0.84 (95% CI 0.79–0.88) of diagnosis for early HCC in the test set.

Conclusions: Our model based on the six-CpG-scorer was a reliable diagnosis tool for early HCC from HBVLD. The usage of the MBS method can realize large-scale detection of CpG sites in clinical diagnosis of early HCC and benefit the majority of patients.

Keywords: multiplex bisulfite sequencing, CpG methylation, early HCC, diagnostic model, enhanced bootstrap validation

INTRODUCTION

Hepatocellular carcinoma (HCC) is the most common primary liver tumor with high morbidity and mortality. It has been estimated that hepatitis B virus (HBV) infection causes 50%–80% of HCC cases worldwide (1). The progression of multi-stage hepatocarcinogenesis from chronic HBV infection (CHB) to HBV-related liver cirrhosis (LC) and finally to HBV-related HCC is complex. There is 2%–7% incidence of LC per year in CHB patients (2), and 2%–4% annual incidence of HCC in LC patients (3). Meanwhile, CHB patients can also develop HCC without cirrhosis. The new data show that annual HCC rates ranged 0.03%–1.57% among non-LC Asian CHB male patients (4). In involving 34,952 patients, the study suggested that 2.29% of CHB patients would develop HCC despite hepatitis B surface antigen (HBsAg) seroclearance (5). There are several mechanisms related with HBV-related hepatocarcinogenesis progression including viral regulatory HBV \times protein interrupting liver cell proliferation and increasing HBV replication (6), integration of HBV DNA into the host cell genome provoking host cell chromosomal alterations and insertional mutagenesis of cancer genes (7), and host genomic and epigenetic aberrant variation induced by inflammation (8).

The high mortality rate of HCC is mostly due to its discovery at advanced stages. There is an urgent unmet need for biomarkers that can detect early HCC development in CHB and LC liver background. DNA methylation profiles for early stage of HCC in peripheral blood mononuclear cells (PBMC) are different from healthy controls as well as CHB. HCC has a specific DNA methylation signature in easily accessible PBMC and can serve as “noninvasive” biomarkers for detection of early HCC as well as HCC progression (9). Several studies have demonstrated CpG methylation prepared for constructing diagnostic, prognostic, and recurrence models for HCC (10–12).

However, in these models, measurement methylation of CpGs was performed by pyrosequencing or methylation specific PCR. These methods were laborious and involved fussy work (13) for detection methylation of dozens of CpGs and inevitable increase of inter-batch differences in large samples. This could cause adverse effects on the diagnostic efficacy of the model.

Therefore, in this study, we applied multiplex bisulfite sequencing (MBS), which is based on the next-generation sequencing (NGS) method to assess the methylation status of 34 CpGs in 654 samples at the same time. Multivariable methods identified a minimal set of CpGs to achieve optimal prediction. Meanwhile, we handled multiple imputation to complete missing data and bootstrapped training datasets for backward feature selection. The model incorporated both the six-CpG-scorer

methylation panel and demographic and clinical characteristics risk factors for early diagnosis onset of HCC from HBV-related liver disease (HBVLD) including CHB and LC.

MATERIALS AND METHODS

Data Processing for CpG Selection

The raw IDAT files of Illumina 450K Beadchip data including CHB patients ($n = 10$) and Barcelona clinic liver cancer staging system (BCLC) 0 ($n = 10$), BCLC-A ($n = 10$), BCLC-B ($n = 10$), and BCLC-C ($n = 9$) were obtained from Gene Expression Omnibus (accession number: GSE67170) (9), which was prepared to obtain differentially methylated CpGs between CHB and each HCC stage. Forty-four paired PBMC samples were taken from 22 patients before and again after diagnosis of HCC. The 22 patients were diagnosed as LC prior to HCC, and then 5 were diagnosed as HCC BCLC-0 and 17 were BCLC-A. Twenty-two LC and 22 early HCC PBMC samples were subjected to genome-wide DNA methylation assay by using Illumina EPIC Beadchip (data did not published). The R package ChAMP was applied for methylation raw data processing and the paired t tests were used to analyze the differentially methylated CpGs between LC and HCC BCLC-0 and -A. The differentially methylated CpGs with $|\Delta \beta| \geq 0.2$ and remaining significant after Bonferroni-corrected p value < 0.05 were selected.

Patient Study Population

The cross-sectional retrospective study, using the convenient sampling method, was conducted from August 2010 to July 2019 at Beijing You’An Hospital, which is an infectious diseases specialist tertiary hospital in China. A total of 654 patients were included in this study. The demographic and clinical characteristic data of patients with CHB, LC, and early HCC were collected from hospital electronic medical records. The inclusion criterion of CHB was that hepatitis B surface antigen (HBsAg) seropositive status lasted at 6 months or beyond according to the Asia-Pacific clinical practice guidelines on the management of hepatitis B: a 2015 update (14). Diagnosis of hepatitis B-related LC was based on a combination of clinical, laboratory, imaging features, and liver biopsies according to the guideline of prevention and treatment for chronic hepatitis B (2010 Version). Diagnosis of HCC was based on the radiological/histological criteria according to 2012 EASL clinical practice guidelines: Management of chronic hepatitis B virus infection, Barcelona clinic liver cancer staging system (BCLC) (15). Exclusion criteria were as follows: less than 18 years old; co-infection with human immunodeficiency virus, hepatitis C virus,

or hepatitis D virus; coexistence of liver injury caused by drug intake, alcohol consumption, and autoimmune hepatitis; pregnancy; and lactation. The study was approved by the Institutional Ethics Committee of the Beijing You'An Hospital. All participants signed written informed consent on enrolment.

DNA Bisulfite Converted and Multiplex Bisulfite Sequencing

After extraction, PBMC DNA bisulfite was converted with sodium bisulfite according to the protocol of EZ DNA Methylation-Direct Kit (ZYMO Research, Irvine, USA), whose bisulfite conversion rate was >99.5%. Bisulfite-transformed DNA was a single strand and we measured the concentration of the single-strand DNA using a Qubit 2.0 (Thermo, USA, catalog Q10212) to ensure that adequate amounts of single-template DNA were invested for library construction. A panel contained 34 "CpG-free" primer pairs designed to target all candidate CpGs. Library preparation was performed by nest-PCR. First-round PCR reaction was set up as follows: bisulfite converted DNA 5 μ l; forward primer mix (10 μ M) 1 μ l; reverse primer mix (10 μ M) 1 μ l; 2 \times PCR Ready Mix 15 μ l (total 25 μ l) (KAPA HiFi HotStart ReadyMix PCR). The plate was sealed and PCR was performed in a thermal instrument (BIO-RAD, T100TM) using the following program: 1 cycle of denaturing at 98°C for 3 min, then 27 cycles of denaturing at 98°C for 20 s, annealing at 60°C for 4 min, and final elongation at 72°C for 2 min. Finally, hold at 10°C. The PCR products were checked using electrophoresis in 1% (w/v) agarose gels in TBE buffer (Tris, boric acid, EDTA) stained with ethidium bromide (EB) and visualized under UV light. Then, we used AMPure XP beads to purify the amplicon product. After that, the second-round PCR was performed. PCR reaction was set up as follows: first-round PCR amplicon product (10 ng/ μ l) 2 μ l; universal P7 primer with barcode (10 μ M) 1 μ l; universal P5 primer with barcode (10 μ M) 1 μ l; 2 \times PCR Ready Mix 15 μ l (total 30 μ l) (Kapa HiFi Ready Mix). The plate was sealed and PCR was performed in a thermal instrument (BIO-RAD, T100TM) using the following program: 1 cycle of denaturing at 98°C for 1 min, then eight cycles of denaturing at 98°C for 20 s, annealing at 60°C for 20 s, elongation at 72°C for 30 s, and a final extension at 72°C for 2 min. Then, we used AMPure XP beads to purify the second-round PCR amplicon product. The libraries were then quantified and pooled. Paired-end sequencing of the library was performed on the HiSeq XTen sequencers (Illumina, San Diego, CA).

Data QC and SNP Calling

MBS raw data were processed by Sangon Biotech. Briefly, raw reads were filtered according to three steps: (a) removing adaptor sequence if reads contains by cutadapt (v 1.2.1); (b) removing low quality bases from reads 3' to 5' ($Q < 20$) by PRINSEQ-lite (v 0.20.3); (c) Bismark (version v0.22.1) (www.bioinformatics.babraham.ac.uk/projects/) was used for CpGs detected with default parameters.

CpG Selection and Assessment

A multi-CpG-based scorer was constructed to diagnose the early HCC patients from HBVLD in the training dataset. The least

absolute shrinkage and selection operator (LASSO) with cross-validation method was applied to select the most significant CpGs from the 34 described in **Supplementary Table S1**. The process was mainly performed using the "glmnet" package (16) based on the R software (Version 4.0.3) and depicted in **Figure 1A**.

Statistical Analysis

Firstly, the restricted cubic splines (RCS) were applied to detect the possible nonlinear dependency of the relationship between early HCC and 17 continuous variables, using three knots at the 25th, 50th, and 75th percentiles of the corresponding variable. There were potential threshold associations between early HCC and five indices [age, direct bilirubin (DBil), total protein (TP), albumin (ALB), and hemoglobin] (p -value for nonlinear < 0.001). We have categorized age to the following groups: <43 years and \geq 43 years, DBil to <7 μ mol/L and \geq 7 μ mol/L, TP to <65 g/L and \geq 65 g/L, ALB to <42 g/L and \geq 42 g/L, and hemoglobin to <140 g/L and \geq 140 g/L based on the RCS curve. The other four indices [total bilirubin (TBil), γ -glutamyltranspeptidase (γ -GT), platelet count (PLT), and lymphocyte count (LYM)] were categorized to normal and abnormal groups based on the medical reference value, respectively. The other seven indices [alanine aminotransferase (ALT), aspartate aminotransferase (AST), alkaline phosphatase (ALP), white blood cell count (WBC), monocyte count (MONO), neutrophil count (NUET), and alpha-fetoprotein (AFP)] were log-transformed, respectively (**Supplementary Table S1**).

Missing values in original dataset were imputed 20 times using imputation with predictive mean matching ("mice" package) (17). For each of the 20 complete dataset, 500 bootstrapping datasets were generated, and backwards feature selection with the Akaike Information Criterion (AIC) was performed on the 10,000 datasets ("rms") (18). Second-order interaction terms were also tested for inclusion. The selected predictors constructed the final model, whose regression coefficients were calculated using "psfmi" package according to "Rubin's Rules" (19, 20). The enhanced bootstrap method was to evaluate the stability of the diagnosis model. Discrimination ability was assessed by the area under the receiver operating characteristic curve (AUROC) and C-statistics. Calibration was applied for assessment of agreement between predicted and observed risks across of the population. The nomogram presented the results of the modeling process. Decision curve analysis (DCA) was performed to determine the model clinical usefulness. The construction process referred to this report (21) and the model analysis conforms to the reporting standards of STARD (22) and was depicted in **Figure 1B**.

RESULTS

Demographic and Characteristics of the Patients

After a strict pathological diagnosis and exclusion process, 168 patients with CHB, 173 patients with liver cirrhosis, 148 patients with HCC BCLC-0 stage, and 165 patients with HCC BCLC-A stage were collected in Beijing You'An hospital and included into this study (**Figure 1A**). A total of 654 patients were randomly assigned

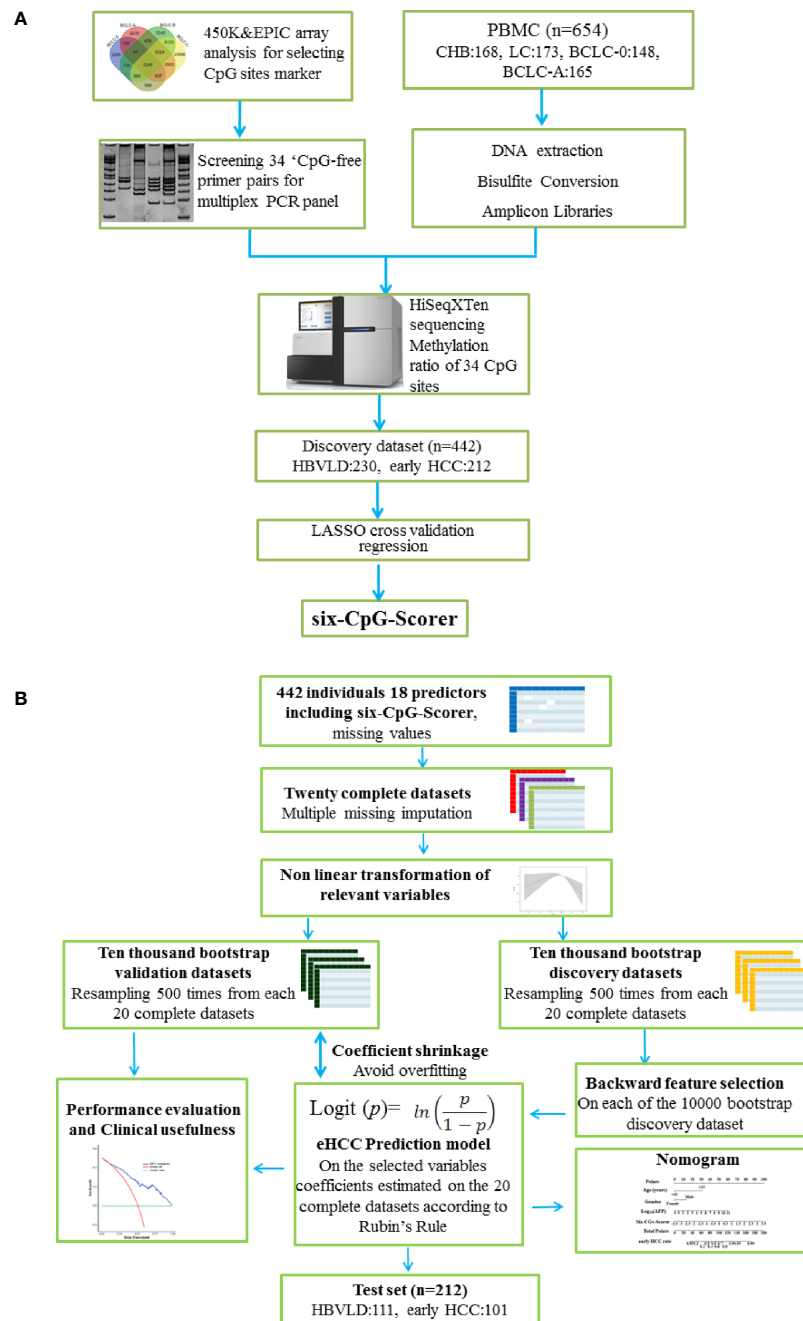


FIGURE 1 | Study design and analysis protocol. **(A)** Study design and flow diagram. A total of 654 PBMC samples were prospectively collected. Thirty-four CpGs were investigated using multiplex bisulfite sequencing in 341 HBVLD (CHB: 168, LC: 173) and 313 early HCC group (BCLC-0:148, BCLC-A: 165). The least absolute shrinkage and selection operator method (LASSO) cross-validation was introduced to selected six CpGs and built a six-CpG-scorer in the training dataset ($n = 442$, 212 early HCC and 230 HBVLD). **(B)** Schematic representation of statistical analysis. The analyses were performed on 18 selected predictors measured on 442 parents involved in the training set. Twenty complete datasets were created after 20 times missing imputation, and 17 candidate variables were detected the possible nonlinear dependency of the relationship with early HCC, of which 7 variables were transformed in a non-linear fashion. Resampling 500 times were from each of the 20 complete datasets, leading to a total number of 10,000 bootstrap datasets. A backward feature selection with AIC was repeated on each of the 10,000 bootstrap datasets for selecting the most relevant risk variables for early HCC. The factors chosen at least once during the feature selection procedure constituted the final mode, whose coefficients were estimated using Rubin's Rule from the 20 complete datasets. In internal validation, the model predictiveness and correcting overfit were assessed using 10,000 separate enhanced bootstrapped datasets. The nomogram presented the final mode. Decision curve analysis and clinical impact curves were performed to determine the final model clinical usefulness. The final mode also showed an obvious diagnosis potential in test set ($n = 212$, 101 early HCC and 111 HBVLD). HBVLD, HBV-related liver disease; HCC, hepatocellular carcinoma; BCLC, Barcelona Clinic Liver Cancer staging system.

to the training set ($n = 442$) and test set ($n = 212$). Demographic and clinical characteristics of patients are shown in **Table 1**.

CpG Selection and Panel Signature Building for Early HCC Diagnosis

On the basis of our previous studies (9), we portrayed differentially methylated CpGs between CHB and each of the

HCC phases utilizing Limma package with Bonferroni correction. The number of specifically methylated CpGs between CHB and each of the HCC phases included 2,285 for BCLC-0; 2,233 for BCLC-A; 3,345 for BCLC-B; and 23,596 for BCLC-C. There were 326 differentially methylated CpGs that could specifically distinguish early HCC (BCLC-0 and BCLC-A stages) from CHB (**Figure 2A**). Moreover, 20 robust CpG

TABLE 1 | Clinical characteristics of the enrolled participants in this study ($n = 654$).

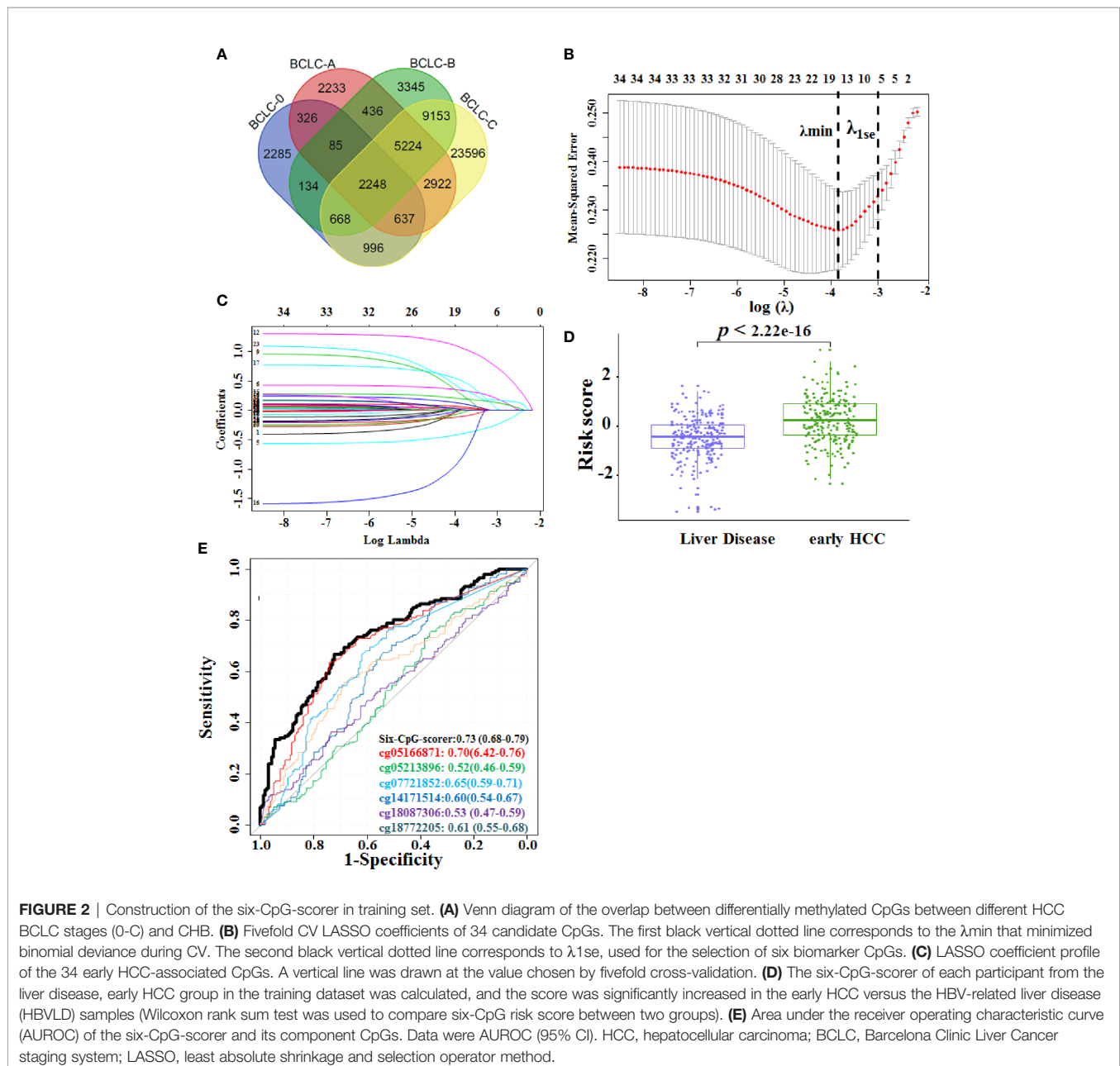
	Training set (442)		Test set (212)	
	HBVLD ($n = 230$)	Early HCC ($n = 212$)	HBVLD ($n = 111$)	Early HCC ($n = 101$)
Age (years, mean \pm SD)	45.37 \pm 11.9	46.22 \pm 11.7	45.38 \pm 12.08	52.24 \pm 10.36
Sex (M/F)	170/60	174/38	80/31	90/11
ALT (U/L)				
<40	108 (47.0%)	128 (60.4%)	51 (45.9%)	60 (59.4%)
\geq 40	121 (52.6%)	83 (39.2%)	60 (54.1%)	41 (40.6%)
AST (U/L)				
<40	125 (54.3%)	140 (66.0%)	59 (53.2%)	55 (54.5%)
\geq 40	104 (45.2%)	71 (30.9%)	52 (46.8%)	46 (44.5%)
Total bilirubin (μ mol/L)				
<21	144 (62.6%)	147 (69.3%)	79 (71.1%)	63 (62.4%)
\geq 21	85 (37.0%)	64 (30.2%)	32 (18.9%)	38 (37.6%)
Direct bilirubin (μ mol/L)				
<7	169 (73.5%)	175 (82.5%)	88 (79.3%)	72 (71.3%)
\geq 7	60 (26.1%)	36 (17.0%)	23 (20.7%)	29 (28.7%)
Total protein (g/L)				
<65	168 (73.4%)	135 (59.0%)	85 (76.6%)	65 (64.4%)
\geq 65	61 (26.5%)	76 (35.8%)	26 (23.4%)	36 (35.6%)
Albumin (g/L)				
<40	136 (59.1%)	105 (49.5%)	72 (64.9%)	45 (44.6%)
\geq 40	93 (40.4%)	106 (50.0%)	39 (35.1%)	56 (55.4%)
γ -GT (U/L)				
<45	121 (52.6%)	95 (44.8%)	52 (46.8%)	40 (39.6%)
\geq 45	96 (41.7%)	95 (44.8%)	52 (46.8%)	61 (60.4%)
Alkaline phosphatase (U/L)				
\leq 100	172 (74.8%)	142 (67.0%)	83 (74.8%)	48 (47.5%)
>100	46 (20.0%)	48 (22.6%)	22 (19.8%)	37 (36.6%)
WBC count $\times 10^9/L$				
<3.5	174 (75.7%)	157 (74.1%)	79 (71.2%)	74 (73.3%)
3.5–9.5	46 (20.0%)	42 (19.8%)	24 (21.6%)	14 (13.9%)
>9.5	10 (4.3%)	12 (5.7%)	8 (7.2%)	13 (12.9%)
Hemoglobin (g/L)				
<130	143 (62.2%)	138 (65.1%)	77 (69.4%)	60 (59.4%)
\geq 130	87 (37.8%)	73 (34.4%)	34 (30.6%)	41 (40.6%)
Platelet count $\times 10^9/L$				
<125	129 (56.1%)	108 (50.9%)	70 (63.1%)	58 (57.4%)
\geq 125	101 (43.9%)	104 (49.1%)	41 (36.9%)	43 (42.6%)
Lymphocyte count $\times 10^9/L$				
<1.1	172 (74.8%)	149 (70.3%)	85 (76.6%)	58 (57.4%)
\geq 1.1	58 (25.2%)	62 (29.2%)	26 (23.4%)	43 (42.6%)
Monocyte count $\times 10^9/L$				
<0.6	214 (93.1%)	182 (85.8%)	107 (96.4%)	81 (80.2%)
\geq 0.6	16 (6.9%)	29 (13.7%)	4 (3.6%)	20 (19.8%)
Neutrophil count $\times 10^9/L$				
<1.8	166 (72.2%)	167 (78.8%)	80 (72.1%)	71 (70.3%)
1.8–6.3	53 (23.0%)	17 (8.0%)	26 (23.4%)	12 (11.9%)
>6.3	11 (4.8%)	17 (8.0%)	5 (4.5%)	18 (17.8%)
Alpha-fetoprotein (ng/ml)				
<20	178 (77.4%)	110 (51.9%)	86 (77.5%)	41 (40.6%)
\geq 20	50 (21.7%)	96 (45.3%)	25 (22.5%)	58 (57.4%)

HBVLD, HBV-related liver disease; CHB, chronic hepatitis B; LC, HBV-related liver cirrhosis; HCC, hepatocellular carcinoma; BCLC, Barcelona clinic liver cancer staging system; γ -GT, γ -glutamyltransferase; WBC, white blood cell. ALT, alanine aminotransferase; AST, aspartate aminotransferase.

differentially methylated sites were used in this study from 33 CpGs ($|\Delta\beta| \geq 0.2$). Meanwhile, 36 differentially methylated CpGs ($|\Delta\beta| \geq 0.2$) could specifically distinguish early HCC from LC using paired t tests with Bonferroni correction, and 17 CpGs were selected for this study (unpublished work). In all, methylation ratios of 34 CpGs (three CpGs overlap) were investigated using MBS in the HBVLD and early HCC samples (**Supplementary Tables S2, S3**).

Thirty-four CpGs were reduced to six potential predictors using the LASSO regression model. The cross-validated error plot and a coefficient profile plot of the LASSO regression model were produced (**Figures 2B, C**). The logistic regression was used

for building the six-CpG-scorer: where risk score = $-0.87 - 3.73 \times \text{cg14171514} + 2.58 \times \text{cg07721852} + 6.91 \times \text{cg05166871} - 9.85 \times \text{cg18087306} + 4.50 \times \text{cg05213896} + 4.39 \times \text{cg18772205}$, where values of each CpG were methylation ratio measured from MBS. We then applied this formula to calculate the risk score for early HCC of each patient based on their individual six CpG methylation ratio. The risk score was significantly increased in the early HCC samples versus the HBVLD samples ($p < 2.22 \times 10^{-16}$) (**Figure 2D**). The six CpGs and their combination six-CpG-scorer also showed diagnostic accuracy (**Figure 2E** and **Supplementary Table S4**). According to determining of maximum Youden index, 0 served as the optimal cutoff point of risk score. Therefore, we classified those patients with risk



score < 0 as low-risk group, and those with risk score ≥ 0 as high-risk group. The distribution of demographic and clinical characteristics did not vary significantly between the high-risk and low-risk group (Supplementary Table S5).

Six-CpG-Scorer Signature Was Independent of Clinical Factors

The univariate logistic analysis was performed in 10,000 bootstrap datasets. Six of the 18 candidate variables indicated a higher early HCC risk; among these were higher age (≥ 43 years), male, individuals with higher AFP, higher six-CpG-scorer, lower TP (< 65 g/L), and lower TBil (Table 2).

Four variables were selected by the backward feature selection procedure in 10,000 bootstrap datasets (Table 2). Age, sex, AFP, and six-CpG-scorer signature were independent risk factors for early HCC. The six-CpG-scorer also showed significantly higher predictive accuracy than AFP (Supplementary Table S6) and other demographic and clinical risk factors.

Development of an Individualized Early HCC Diagnosis Nomogram

The early HCC diagnosis model incorporated the four risk predictors and estimated on the 20 complete datasets according to Rubin's Rule. The prognostic index X (based on logistic regression model coefficients) was: $X = -1.0944708 - 0.7183741 \times \text{Sex (Male} = 0, \text{Female} = 1) + 1.7286974 \times \text{Age } [(< 43 \text{ years}) = 0, (\geq 43 \text{ years}) = 1] + 0.2761166 \times \lg(\text{AFP}) + 0.7902764 \times \text{six-CpG-scorer}$. The calculation of the predicted risk of early HCC from HBVLD was as follows: risk of eHCC = $\frac{1}{1 + \exp(-X)}$. It presented as the early HCC nomogram (eHCC nomogram) (Figure 3A).

Estimation for the C-Statistics and Brier Score by Bootstrap Validation

Internal validation was performed using the 500 times resampling enhanced bootstrap method from each of the 20 complete datasets. The result showed negligible model optimism. The apparent C-statistics and apparent Brier score was 0.805 and 0.200, respectively. The optimism of the C-statistics and Brier score was -0.0042 and 0.00164 , respectively. The adjusted C-statistics and Brier score was 0.809 and 0.199, respectively.

Diagnostic Performance and Clinical Usefulness of eHCC Nomogram

The AUROC of the model was 0.81 (95% CI, 0.77–0.85) in the training set. The sensitivity, specificity, positive predictive value (PPV), and negative predictive value (NPV) when used in differentiating the early HCC from HBVLD were 70.0%, 77.8%, 74.4%, and 73.6%, respectively. The calibration curve of the eHCC nomogram for the probability of early HCC demonstrated good agreement between prediction and observation in the training set (Figure 3B). The decision curve analysis of the eHCC nomogram and that for the model without the six-CpG-scorer is presented in Figure 3C. The DCA showed that if the threshold probability of a patient or doctor was $> 10\%$, using eHCC nomogram to predict early HCC adds more benefit than either the treat-all-patients scheme or the treat-none scheme (Figure 3D).

Diagnostic Performance of the eHCC Nomogram in the Test Set

We further enrolled 212 patients including 111 HBVLD and 101 early HCC to serve as the test set for validation of the diagnostic potential. The risk score was significantly increased in the early HCC versus the HBVLD group in the test set ($p = 2.7 \times 10^{-7}$).

TABLE 2 | All 18 variables included in the backwards feature selection analysis.

Variable	Univariable		Multivariable	
	OR (95% CI)	p-value	OR (95% CI)	p-value
Age (years), ≥ 43 vs. < 43	5.07 (3.07–8.56)	1.75e-07***	5.23 (3.24–8.63)	2.56e-08***
Sex (Female vs. Male)	0.32 (0.17–0.56)	0.0011**	0.32 (0.19–0.53)	0.000248***
Alpha-fetoprotein (AFP) (ng/ml), \log_{10}^a	1.50 (1.35–1.69)	1.85e-09***	1.48 (1.34–1.64)	3.05e-10***
Six-CpG-Scorer	2.37(1.83–3.12)	1.10e-07***	2.58 (2.01–3.36)	1.08e-09***
Total protein(g/L), ≥ 65 vs. < 65	0.38 (0.19–0.71)	0.01209*	0.32 (0.20–0.51)	0.56
Total bilirubin($\mu\text{mol/L}$), ≥ 21 vs. < 21	0.32 (0.14–0.69)	0.01588*	0.45 (0.32–0.64)	0.78
AST (U/L), \log_{10}	0.77 (0.45–1.28)	0.40551		
ALT (U/L), \log_{10}	0.51(0.43–1.06)	0.15320		
Direct bilirubin ($\mu\text{mol/L}$), ≥ 7 vs. < 7	0.55 (0.77–2.35)	0.38832		
γ -GT (U/L), ≥ 45 vs. < 45	1.15 (0.83–1.61)	0.47649		
Albumin (g/L), ≥ 40 vs. < 40	0.74 (0.41–1.36)	0.42147		
Alkaline phosphatase (U/L), \log_{10}	0.77 (0.44–1.35)	0.44623		
Hemoglobin (g/L), ≥ 115 vs. < 115	1.68 (0.91–3.14)	0.16827		
White blood cell count $\times 10^9/\text{L}$, \log_{10}	0.84 (0.17–4.24)	0.85430		
Monocyte count $\times 10^9/\text{L}$, truncate _{.99} + \log_{10}^b	2.29 (1.14–4.67)	0.05410.		
Platelet count $\times 10^9/\text{L}$, ≥ 125 vs. < 125	0.84(0.50–1.42)	0.58796		
Lymphocyte count $\times 10^9/\text{L}$, ≥ 1.1 vs. < 1.1	0.82 (0.46–1.49)	0.58026		
Neutrophil count $\times 10^9/\text{L}$, \log_{10}	1.08 (0.37–2.86)	0.89871		

^aNonlinear transformation.

^bMonocyte count variable was truncated with 1st and 99th percentiles and then performed with nonlinear transformation.

OR, odds ratio; γ -GT, γ -glutamyltranspeptidase; ALT, alanine aminotransferase; AST, aspartate aminotransferase. Signif. codes: **** 0.001, **** 0.01, *** 0.05.

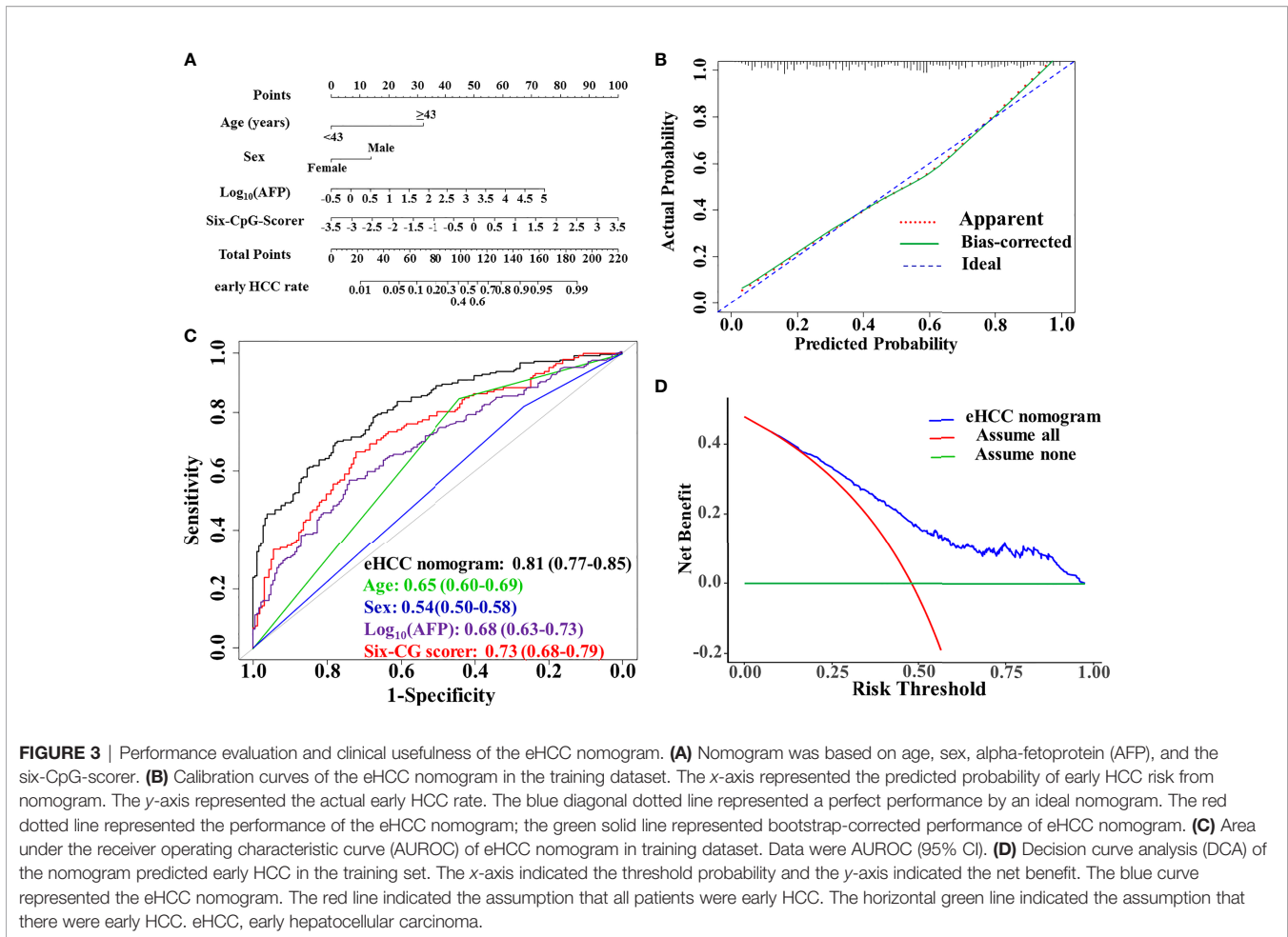


(Figure 4A). The eHCC nomogram achieved an AUROC value of 0.84 (95% CI 0.79–0.88) between the early HCC and HBVLD (Figure 4B). The calibration curve demonstrated good agreement between prediction and observation in early HCC (Figure 4C). The sensitivity, specificity, PPV, and NPV were used in differentiating the early HCC from HBVLD and were 68.9%, 82.9%, 80.0%, and 71.8%, respectively. The nomogram also indicated good clinical benefits in DCA, which suggested an obvious diagnosis efficacy for early HCC from HBVLD (Figure 4D).

DISCUSSION

The identification of differentially methylated CpG genome-wide from the Methylation Chip (450K and EPIC) often required a test and/or replication in extra cohorts. The pyrosequencing, bisulfite-conversion-based methylation PCR, PCR cloning, and Sanger sequencing method were laborious and involved fussy work for detection methylation of each CpG site and inevitable increase of inter-batch differences in large samples. The deep sequencing of specific target CpGs often called for MBS, which is

based on the NGS method to assess the methylation status at target DNA regions and with very high coverage (13). The important and commendable characteristics of MBS were low cost, low DNA input, and high repeatability and scalability. In addition, the MBS was compatible with common NGS platforms using standard equipment, making it available to most laboratories (23). Construction of amplicon libraries according to a target CpG panel was a key step of MBS. In multiplex PCR using bisulfite converted DNA as template, mixed-base primers, whose pyrimidine base Y contains a “mixture” of cytosines and thymines at the cytosine site and whose purine base R contains a mixture of guanines and adenines at the guanine site, greatly affected the amplification efficiency and led to a decrease in library quality. In the design of this study, we applied 34 “CpG-free” primer pairs (i.e., primers that do not bind to a region containing CpG dinucleotides) targeting each region covering candidate CpGs, which had been considered to produce “non-preferential” amplification of bisulfite-converted DNA genome (24). We successfully establish a version of the “CpG-free” primer pair panel applied in MBS to simultaneously investigate the methylation status of 34 candidate CpGs across a large sample size ($n = 654$). The complete and accurate methylation

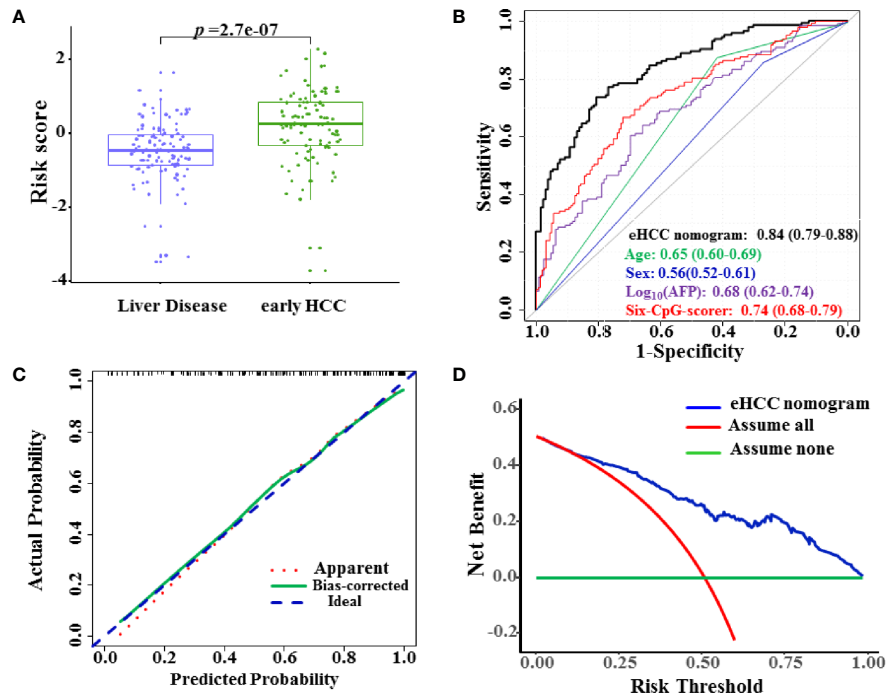


FIGURE 4 | Diagnostic performance of the eHCC nomogram in the test set. **(A)** The risk score was significantly increased in the early HCC samples versus the HBVLD group ($p = 2.7 \times 10^{-7}$). **(B)** Area under the receiver operating characteristic curve (AUROC) of eHCC nomogram in the test set. Data were AUROC (95% CI). **(C)** Calibration curves of the eHCC nomogram in the test set. The x-axis represented the predicted probability of HCC risk from nomogram. The y-axis represented the actual HCC rate. The blue diagonal dotted line represented a perfect performance by an ideal nomogram. The red dotted line represented the performance of the eHCC nomogram, and the green solid line represented bootstrap-corrected performance of eHCC nomogram. **(D)** Decision curve analysis (DCA) of the nomogram predicted early HCC in the test set. The x-axis indicated the threshold probability, and the y-axis indicated the net benefit. The blue curve represented the eHCC nomogram. The red line indicated the assumption that all patients were HCC. The horizontal green line indicated the assumption that there were early HCC. eHCC, early hepatocellular carcinoma.

data of 34 candidate CpGs allowed us to screen out and integrate into a six-CpG-scorer with application of LASSO regression.

CpG methylation served as an apparatus focused on non-invasive biomarkers for chronic diseases {age-related diabetes (25), diabetic embryopathy (26), coronary heart disease (27), nonalcoholic fatty liver disease (28), or cancer [bladder cancer (29), rectal cancer (30), and HCC (31)]} and had been set up by compelling studies. Our recent study looked at CpG methylation alterations of HBV-related liver disease and developed a model discriminating compensated cirrhosis patients from CHB and decompensated cirrhosis ones based on two CpG biomarkers (32). Our previous study also supported the feasibility of using 350 CpGs for detection of each stages of HCC from healthy control (9). In this study, we successfully established and validated a novel diagnostic nomogram based on the six-CpG-scorer to distinguish early HCC patients from CHB and LC ones. Furthermore, this proposed six-CpG-scorer can diagnose the early HCC better than other demographic and characteristics risk factors. Meanwhile, eHCC nomogram validated considerable diagnostic potential to early HCC and indicated good clinical benefits in DCA.

The CpGs serving as independent risk factors of HCC from mining analysis of Methylation Chip data might point out a novel trace for the exploration of HCC progress mechanism. Based on the

Illumina Human Beadchip 27K array, sphingomyelin phosphodiesterase 3 (SMPD3) and neurofilament, heavy polypeptide (NEFH) were found to behave as tumor suppressor genes in HCC after validation *in vitro* and *in vivo* (33). Gentilini et al. applied the Methylation 450K BeadChip array and showed that four epigenetically regulated candidate genes [adherens junction associated protein 1 (AJAP1), adenosine deaminase RNA specific B2 (ADARB2), protein tyrosine phosphatase receptor type N2 (PTPRN2), and sidekick cell adhesion molecule 1 (SDK1)] were potentially involved in the pathogenesis of HCC (34). The finding of AJAP1 was consistent with clinical observation of low AJAP1 expression as an independent factor for predicting disease-free survival (DFS) (35). Mechanically, AJAP1 could block epithelial-to-mesenchymal transition (EMT) *via* suppressing β -catenin/zinc finger E-box binding homeobox 1 (ZEB1) signaling.

In this study, cg14171514 was located within the 5'UTR of the neuroblast differentiation-associated protein (AHNAK) gene, and significantly hypomethylated both in the PBMC DNA of early HCC patients compared with HBVLD ones in this study. Consistently, the aberrant hypomethylation status in the AHNAK gene promoter region from HCC patients' PBMC DNA was verified in methylation-specific PCR (MSP) results of our previous studies (36). Aberrant AHNAK methylation level

in PBMC DNA was associated with HCC. In addition, AHNAK mRNA had been reported to be overexpressed in liver cancer tissues by qPCR (36) and the cancer genome atlas (TCGA) data (**Supplementary Figure S1**). Our novel results from immunoprecipitation in combination with mass spectrometry (IP-MS) analysis strongly indicated that AHNAK protein was involved in and promoted HCC progress (data not published). The cg18087306 was located within the body of Lamin B2 (LMNB2) gene, whose expression level in HCC tissue was higher relative to peritumor tissue. LMNB2 was a promising HCC prognostic and diagnostic biomarker (37).

CONCLUSIONS

We had shown characteristic changes of 34 CpGs in HBVLD and early HCC across a clinical cohort, identified the six-CpG-scorer, and validated their diagnostic efficacy. Thus, we proposed that the six-CpG-scorer-based nomogram is a potential non-invasive diagnostic tool for early HCC from HBVLD, and performed internal validation using the 500 times resampling enhanced bootstrap method from each of the 20 complete datasets to evaluate the stability and then applied it to the test set for validation. The external validation of the nomogram will be needed in much larger cohorts from different centers or regions to promote the efficacy and stability to further benefit HCC populations.

DATA AVAILABILITY STATEMENT

The datasets presented in this study can be found in online repositories. The names of the repository/repositories and accession number(s) can be found in the article/**Supplementary Material**.

REFERENCES

- Venook AP, Papandreou C, Furuse J, Ladrón de Guevara L. The Incidence and Epidemiology of Hepatocellular Carcinoma: A Global and Regional Perspective. *Oncol* (2010) 15(S4):5–13. doi: 10.1634/theoncologist.2010-S4-05
- Hsu YS, Chien RN, Yeh CT, Sheen IS, Chiou HY, Chu CM, et al. Long-Term Outcome After Spontaneous HBeAg Seroconversion in Patients With Chronic Hepatitis B. *Hepatology* (2002) 35(6):1522–7. doi: 10.1053/jhep.2002.33638
- El-Serag HB. Hepatocellular Carcinoma. *N Engl J Med* (2011) 365(12):1118–27. doi: 10.1056/NEJMra1001683
- Liu M, Tseng T-C, Jun DW, Yeh M-L, Trinh H, Wong GLH, et al. Transition Rates to Cirrhosis and Liver Cancer by Age, Gender, Disease and Treatment Status in Asian Chronic Hepatitis B Patients. *Hepatol Int* (2021) 15:71–81. doi: 10.1007/s12072-020-10113-2
- Liu F, Wang X-W, Chen L, Hu P, Ren H, Hu H-D. Systematic Review With Meta-Analysis: Development of Hepatocellular Carcinoma in Chronic Hepatitis B Patients With Hepatitis B Surface Antigen Seroclearance. *Aliment Pharmacol Ther* (2016) 43(12):1253–61. doi: 10.1111/apt.13634
- Guerrieri F, Belloni L, D'Andrea D, Pediconi N, Le Pera L, Testoni B, et al. Genome-Wide Identification of Direct HBx Genomic Targets. *BMC Genomics* (2017) 18(1):017–3561. doi: 10.1186/s12864-017-3561-5
- Buendia MA, Neuvet C. Hepatocellular Carcinoma. *Cold Spring Harb Perspect Med* (2015) 5(2):a021444. doi: 10.1101/cshperspect.a021444
- Gehring AJ, Ho ZZ, Tan AT, Aung MO, Lee KH, Tan KC, et al. Profile of Tumor Antigen-Specific CD8 T Cells in Patients With Hepatitis B Virus-Related Hepatocellular Carcinoma. *Gastroenterology* (2009) 137(2):682–90. doi: 10.1053/j.gastro.2009.04.045
- Zhang Y, Petropoulos S, Liu J, Cheishvili D, Zhou R, Dymov S, et al. The Signature of Liver Cancer in Immune Cells DNA Methylation. *Clin Epigenetics* (2018) 10(1):8. doi: 10.1186/s13148-017-0436-1
- Long J, Chen P, Lin J, Bai Y, Yang X, Bian J, et al. DNA Methylation-Driven Genes for Constructing Diagnostic, Prognostic, and Recurrence Models for Hepatocellular Carcinoma. *Theranostics* (2019) 9(24):7251–67. doi: 10.7150/thno.31155
- Scusi EL, Loose DS, Wray CJ. Clinical Implications of DNA Methylation in Hepatocellular Carcinoma. *HPB (Oxford)* (2011) 13(6):369–76. doi: 10.1111/j.1477-2574.2011.00303.x
- Jiang HY, Ning G, Wang YS, Lv WB. 14-CpG-Based Signature Improves the Prognosis Prediction of Hepatocellular Carcinoma Patients. *BioMed Res Int* (2020) 8:9762067. doi: 10.1155/2020/9762067
- Rainbow DB, Yang X, Burren O, Pekalski ML, Smyth DJ, Klarqvist MD, et al. Epigenetic Analysis of Regulatory T Cells Using Multiplex Bisulfite Sequencing. *Eur J Immunol* (2015) 45(11):3200–3. doi: 10.1002/eji.201545646
- Sarin SK, Kumar M, Lau GK, Abbas Z, Chan HL, Chen CJ, et al. Asian-Pacific Clinical Practice Guidelines on the Management of Hepatitis B: A 2015 Update. *Hepatol Int* (2016) 10(1):1–98. doi: 10.1007/s12072-015-9675-4

ETHICS STATEMENT

The studies involving human participants were reviewed and approved by Ethics Committee of the Beijing You'An Hospital. The patients/participants provided their written informed consent to participate in this study.

AUTHOR CONTRIBUTIONS

YHZ and KL conceived and designed the experiments. KL, YS, LQ, and AL performed all of the experiments. YS designed multiplex bisulfite sequencing and acquired raw data. KL, LR, and SJ conducted the statistical analysis. KL, LQ, CZ, JS, and YZ contributed to collection and processing of samples. All authors contributed to the article and approved the submitted version.

FUNDING

This project was supported by grants from the National Key R&D Program of China (2020YFE0202400), Beijing Natural Science Foundation (7202069 and 7191004), Capital's Funds of Health Improvement and Research (CFH2020-1-2182 and CFH2020-2-1153), Beijing Municipal Science & Technology Commission (Z171100001017078), and Beijing Key Laboratory (BZ0373).

SUPPLEMENTARY MATERIAL

The Supplementary Material for this article can be found online at: <https://www.frontiersin.org/articles/10.3389/fonc.2021.756326/full#supplementary-material>

15. Liver EAFTSOT. EASL Clinical Practice Guidelines: Management of Chronic Hepatitis B Virus Infection. *J Hepatol* (2012) 57(1):167–85. doi: 10.1016/j.jhep.2012.02.010
16. Friedman J, Hastie T, Tibshirani R. Regularization Paths for Generalized Linear Models via Coordinate Descent. *J Stat Software* (2010) 33(1):1–22. doi: 10.18637/jss.v033.i01
17. van Buuren S, Groothuis-Oudshoorn K. Mice: Multivariate Imputation by Chained Equations in R. *J Stat Software* (2011) 45(3):1–67. doi: 10.18637/jss.v045.i03
18. Harrell FE. Regression Modeling Strategies: With Applications, to Linear Models, Logistic and Ordinal Regression, and Survival Analysis, 2nd Ed. Heidelberg: Springer. *Biometrics* (2016) 72:1006. doi: 10.1111/biom.12569
19. Heymans MW, van Buuren S, Knol DL, van Mechelen W, de Vet HC. Variable Selection Under Multiple Imputation Using the Bootstrap in a Prognostic Study. *BMC Med Res Methodol* (2007) 7(33):1471–2288. doi: 10.1186/1471-2288-7-33
20. Eekhout I, van de Wiel MA, Heymans MW. Methods for Significance Testing of Categorical Covariates in Logistic Regression Models After Multiple Imputation: Power and Applicability Analysis. *BMC Med Res Methodol* (2017) 17(1):129. doi: 10.1186/s12874-017-0404-7
21. Markaki M, Tsamardinos I, Langhammer A, Lagani V, Hveem K, Roe OD. A Validated Clinical Risk Prediction Model for Lung Cancer in Smokers of All Ages and Exposure Types: A HUNT Study. *EBioMedicine* (2018) 31:36–46. doi: 10.1016/j.ebiom.2018.03.027
22. Bossuyt PM, Reitsma JB, Bruns DE, Gatsonis CA, Glasziou PP, Irwig L, et al. STARD 2015: An Updated List of Essential Items for Reporting Diagnostic Accuracy Studies. *BMJ* (2015) 28(351):h5527. doi: 10.1136/bmj.h5527
23. Korbic D, Lin E, Wall D, Nair SS, Stirzaker C, Clark SJ, et al. Multiplex Bisulfite PCR Resequencing of Clinical FFPE DNA. *Clin Epigenetics* (2015) 7(1):15–67. doi: 10.1186/s13148-015-0067-3
24. Clark SJ, Harrison J, Paul CL, Frommer M. High Sensitivity Mapping of Methylated Cytosines. *Nucleic Acids Res* (1994) 22(15):2990–7. doi: 10.1093/nar/22.15.2990
25. Grant CD, Jafari N, Hou L, Li Y, Stewart JD, Zhang G, et al. A Longitudinal Study of DNA Methylation as a Potential Mediator of Age-Related Diabetes Risk. *Geroscience* (2017) 39(5-6):475–89. doi: 10.1007/s11357-017-0001-z
26. Schulze KV, Bhatt A, Azamian MS, Sundgren NC, Zapata GE, Hernandez P, et al. Aberrant DNA Methylation as a Diagnostic Biomarker of Diabetic Embryopathy. *Genet Med* (2019) 21(11):2453–61. doi: 10.1038/s41436-019-0516-z
27. Horvath S, Gurven M, Levine ME, Trumble BC, Kaplan H, Allayee H, et al. An Epigenetic Clock Analysis of Race/Ethnicity, Sex, and Coronary Heart Disease. *Genome Biol* (2016) 17(1):016–1030. doi: 10.1186/s13059-016-1030-0
28. Hyun J, Jung Y. DNA Methylation in Nonalcoholic Fatty Liver Disease. *Int J Mol Sci* (2020) 21:8138. doi: 10.3390/ijms21218138
29. Kitchen MO, Bryan RT, Emes RD, Luscombe CJ, Cheng KK, Zeegers MP, et al. HumanMethylation450K Array-Identified Biomarkers Predict Tumour Recurrence/Progression at Initial Diagnosis of High-Risk Non-Muscle Invasive Bladder Cancer. *biomark Cancer* (2018) 8(10):1179299–17751920. doi: 10.1177/1179299X17751920
30. Exner R, Pulverer W, Diem M, Spaller L, Woltering L, Schreiber M, et al. Potential of DNA Methylation in Rectal Cancer as Diagnostic and Prognostic Biomarkers. *Br J Cancer* (2015) 113(7):1035–45. doi: 10.1038/bjc.2015.303
31. Villanueva A, Portela A, Sayols S, Battiston C, Hoshida Y, Méndez-González J, et al. DNA Methylation-Based Prognosis and Epidrivers in Hepatocellular Carcinoma. *Hepatology* (2015) 61(6):1945–56. doi: 10.1002/hep.27732
32. Li K, Qin L, Jiang S, Li A, Zhang C, Liu G, et al. The Signature of HBV-Related Liver Disease in Peripheral Blood Mononuclear Cell DNA Methylation. *Clin Epigenetics* (2020) 12(1):81. doi: 10.1186/s13148-020-00847-z
33. Revilla K, Wang T, Lachenmayer A, Kojima K, Harrington A, Li J, et al. Genome-Wide Methylation Analysis and Epigenetic Unmasking Identify Tumor Suppressor Genes in Hepatocellular Carcinoma. *Gastroenterology* (2013) 145(6):1424–35. doi: 10.1053/j.gastro.2013.08.055
34. Gentilini D, Scala S, Gaudenzi G, Garagnani P, Capri M, Cescon M, et al. Epigenome-Wide Association Study in Hepatocellular Carcinoma: Identification of Stochastic Epigenetic Mutations Through an Innovative Statistical Approach. *Oncotarget* (2017) 8(26):41890–902. doi: 10.18632/oncotarget.17462
35. Ezaka K, Kanda M, Sugimoto H, Shimizu D, Oya H, Nomoto S, et al. Reduced Expression of Adherens Junctions Associated Protein 1 Predicts Recurrence of Hepatocellular Carcinoma After Curative Hepatectomy. *Ann Surg Oncol* (2015) 22(3):015–4695. doi: 10.1245/s10434-015-4695-9
36. Sun L, Li K, Liu G, Xu Y, Zhang A, Lin D, et al. Distinctive Pattern of AHNK Methylation Level in Peripheral Blood Mononuclear Cells and the Association With HBV-Related Liver Diseases. *Cancer Med* (2018) 7(10):5178–86. doi: 10.1002/cam4.1778
37. Kong W, Wu Z, Yang M, Zuo X, Yin G, Chen W. LMNB2 is a Prognostic Biomarker and Correlated With Immune Infiltrates in Hepatocellular Carcinoma. *IUBMB Life* (2020) 72(12):2672–85. doi: 10.1002/iub.2408

Conflict of Interest: The authors declare that the research was conducted in the absence of any commercial or financial relationships that could be construed as a potential conflict of interest.

Publisher's Note: All claims expressed in this article are solely those of the authors and do not necessarily represent those of their affiliated organizations, or those of the publisher, the editors and the reviewers. Any product that may be evaluated in this article, or claim that may be made by its manufacturer, is not guaranteed or endorsed by the publisher.

Copyright © 2021 Li, Song, Qin, Li, Jiang, Ren, Zang, Sun, Zhao and Zhang. This is an open-access article distributed under the terms of the Creative Commons Attribution License (CC BY). The use, distribution or reproduction in other forums is permitted, provided the original author(s) and the copyright owner(s) are credited and that the original publication in this journal is cited, in accordance with accepted academic practice. No use, distribution or reproduction is permitted which does not comply with these terms.